A Unified Theory for Including Surface Kinetic Effects on Ice Vapor Growth in Cloud Models

Chengzhu Zhang[1]*and Jerry Y. Harrington[1]

[1] *Department of Meteorology, Pennsylvania State University, University Park, PA*

1 Introduction

The growth of ice is an important link in the macrophysical evolution of atmospheric "cold clouds." Unlike liquid drops, ice crystals can grow to large sizes by vapor deposition alone, leading to complex crystalline forms. In fact, the growth of ice depends on crystal shape in important ways, yet it is impossible to capture the complexity of ice as it grows in nature. As a result, a simplified framework that can capture the essence of crystal growth is required for theories, and even simpler methods are needed for numerical cloud models.

In macroscopic cloud evolution, vapor diffusional growth can have strong influences on crystal mass and size, even at sizes where collection and sedimentation become important. It is understood that the vapor growth of ice is a vital link in the chain of cold-cloud evolution, however, important gaps exist in our knowledge of the rates and mechanisms involved. Unfortunately, because cloud microphysical processes are interlinked, uncertainties in the core physics of these processes can directly lead to large variability in predicted cloud structure and lifetime (Starr and Cox, 1985a,b; Harrington et al., 1999; Starr and Co-authors, 2000; Liu et al., 2003; Harrington et al., 2009). Simplicity is therefore essential in order to correct these uncertainties and eventually prevent physical inconsistencies between actual crystal growth, modeled growth, and the evolution of cold clouds.

Modeling the vapor growth of ice is difficult primarily because of the non-spherical ice particle shapes. The shapes of ice crystals are best characterized in terms of their primary and secondary habits. The *primary habit* is defined by the aspect ratio, $\phi = c/a$, where c is the semi-length of the prism face of a hexagonal prism and a is the semi-length of the basal face. Early laboratory results show that the primary habit depends on the temperature. These habits oscillate between plate-like ($\phi < 1$) crystals for T between -1 and -3°C, and -10 and -22°C, and column-like ($\phi > 1$) crystals for T between -3 and -10°C and less than -22°C (e.g. Takahashi et al., 1991; Fukuta and Takahashi, 1999). However, more recent results suggest that both plates and columns can occur at low (< -22°C) temperatures (e.g. Libbrecth, 2003; Bailey and Hallett, 2002, 2004), while some studies suggest that the primary habit at low temperatures is almost always plate-like (Bailey and Hallett, 2009). The *secondary habits* depend on the vapor density of the environment. At low vapor densities, laboratory studies suggest that crystals take on more "perfect" hexagonal forms like plates and columns. However, as vapor densities rise and approach liquid saturation, crystalline forms appear more complex with hollowing resulting, and dendrites or rosettes appearing (Fukuta and Takahashi, 1999). Moreover, many in-situ measurements show irregular crystalline shapes occur frequently in nature (Korolev et al., 1999), such as polycrystals that have formed on frozen drops. Regardless, care must be taken when interpreting both laboratory and in-situ data. Laboratory data provide information in highly controlled situations unlikely to occur in nature. However, this ideality is necessary in order to understand the basic physics of crystal growth. In-situ data provides only an end-point in a diverse chain of processes, and hence it is difficult to know with any certainty what environments to which the resulting measured crystal was exposed. Nevertheless, in-situ data provide a vital snapshot in the evolution of real clouds.

Representing basic crystal shapes in a cloud model poses severe difficulties. It is impossible to solve, with any analytical rigor, the diffusion equations for a non-spherical crystal. However, some progress can be made by assuming a spheroidal crystal shape as exemplified in Chen and Lamb (1994). While atmospheric crystals are certainly never spheroids, the spheroidal shape does allow for an extension of the basic equations for growth from spheres (radius only) to non-spheres (a and c dimensions). Spheroids also allow approximation of the aspect ratio of a large variety of crystalline types, which is advantageous given that crystals sampled in clouds are often irregular (e.g. Korolev et al., 1999). Furthermore, because the capacitance is known analytically for spheroids, the mass diffusion equations can be solved exactly. This is beneficial because changes in primary and secondary habits can be captured to first order by supplementing the diffusion model with a *mass distribution hypothesis* from crystal growth theory which supplies information regarding how the increased mass should be distributed over the a and c-axes (Chen and

* *Corresponding author address*: Chengzhu Zhang, Department of Meteorology, Pennsylvania State University, 503 Walker Building, University Park, PA 16802; *e-mail*: cxz158@psu.edu

Lamb, 1994). Using independently-derived laboratory data, Chen and Lamb (1994) showed that this model can accurately capture the mass and aspect ratio evolution of individual ice crystals. Note that the Chen and Lamb (1994) model is a significant departure from the traditional capacitance model. The model combines traditional *Fickian* diffusion with mass *distribution* from crystal growth theory, and hence is no longer a capacitance model. It is the mass redistribution from crystal growth theory that allows for a freely evolving aspect ratio, whereas the pure capacitance model holds the aspect ratio constant in time (Nelson, 1994). Because of these physical facts, the model is re-termed the *Fickian-distribution model* of ice crystal growth (Sulia et al., 2010).

The method derived by Chen and Lamb (1994) provides perhaps the best method to date for parameterizing the nonlinear evolution of both crystal mass and aspect ratio as a function of temperature: Its simplicity allows for the use in at least one cloud model (Hashino and Tripoli, 2007, 2008) in addition to providing the basis of a parameterization of ice habit evolution for bulk cloud models (Sulia et al., 2010). While simple, Chen and Lamb (1994) is most accurate near liquid saturation making the model most appropriate for mixed-phase clouds.

While accurate at liquid saturation, the traditional Fickian diffusion model fails for ice crystal growth at low ice supersaturations (e.g. Nelson and Baker, 1996; Wood et al., 2001). Methods such as Chen and Lamb (1994) overestimate the mass growth rate because surface kinetic influences on crystal growth are not explicitly included in the theory. Regardless of saturation state, molecules in the vapor phase must find an attachment point on the surface of the ice if the crystal is to grow. Typically, growth is broken down along the two primary axes (a and c) associated with perfect hexagonal prisms. The efficiency of growth along each axis is defined in terms of a *deposition coefficient*, α_a and α_c, which ranges between zero and one: Zero means that no molecules are incorporated and the axis does not grow, whereas a value of one indicates that all molecules that encounter the surface are incorporated, and so the axis grows at its maximum rate. Laboratory data on the growth efficiencies range from particle averaged values (e.g. Magee et al., 2006) to values for each axis (Nelson and Knight, 1998; Libbrecth, 2003); though some of these data do not agree with each other. Some data indicate that growth efficiencies are very high (near one) whereas other data suggest that the deposition coefficient for ice is quite small ($\alpha_d \sim 0.005$) at typical cirrus temperatures (T $\sim$ -50 °C) indicating that ice vapor growth can be strongly limited by surface kinetics (Magee et al., 2006). Unfortunately, no general method exists for the inclusion of the deposition coefficient in theoretical models of ice crystal growth, though some approximations do exist (e.g. Gayet et al., 2002; Harrington et al., 2009). Nevertheless, the prediction of crystal habit has been shown to be critical to mixed-phase cloud evolution (e.g. Avramov and Harrington, 2010) and studies have illustrated the importance of the deposition coefficient for cirrus evolution (e.g. Gayet et al., 2002; Khvorostyanov et al., 2006; Harrington et al., 2009) where dynamic and microphysical processes work in tandem to determine the micro- and macrophysical evolution of the cloud system.

We provide a method for the inclusion of surface kinetics in the Fickian-distribution model of ice crystal growth. First, we review the basics of surface kinetic influences by considering spherical growth. We then introduce our new model along with tests of its relevance for atmospheric conditions.

2 Surface Kinetic Influences on Spherical Vapor Growth

The effects of surface kinetics appear as modifications to the diffusion coefficients in the standard vapor growth equation for an ice sphere:

$$\frac{dm}{dt} = 4\pi C G(T, P, r, \alpha_d) s_i, \tag{1}$$

where s_i is the ice supersaturation, C is the capacitance (which is equal to r for an eqivalent volume sphere), and the combined diffusion coefficient, G, is defined as (Pruppacher and Klett, 1997)

$$G(T, P, r, \alpha_d) = \left[\frac{R_v T}{e_i(T) D_v^*} + \frac{L_s}{K_T^* T} \left(\frac{L_s}{T R_v} - 1 \right)^{1/2} \right]^{-1} \tag{2}$$

where T is temperature, P is pressure, R_v is the vapor gas constant, e_i is the ice equilibirum vapor pressure, L_s is the enthalpy of sublimation, and D_v^* and K_T^* are the kinetically-modified vapor and thermal diffusion coefficients, respectively. For our analysis, we have assumed spherical geometry for simplicity and because it is the method most used in the literature (e.g. Pruppacher and Klett, 1997). The assumption to use equivalent volume or density spheres is necessary for it is unclear how to implement the deposition coefficient, α_d, into the Fickian-distribution model.

The corrections for surface kinetic effects for spherical particles are included through modified vapor and thermal diffusion coefficients via Pruppacher and Klett (1997)

$$D_v^* = \frac{D_v}{\frac{r}{r+\Delta_v} + \frac{l_d}{r}} \qquad \text{and} \qquad K_T^* = \frac{K_T}{\frac{r}{r+\Delta_T} + \frac{l_T}{r}} \tag{3}$$

where Δ_v and Δ_T are the so-called vapor and thermal jump lengths, respectively, and each is proportional to the mean free path. The last two variables, l_d and l_T are interpreted as kinetic length scales (e.g. Mordy, 1959; Pruppacher and Klett, 1997) and are defined as,

$$l_d = \frac{4 D_v}{\alpha_d \overline{v}_v} \qquad \text{where} \qquad \overline{v}_v = \left(\frac{R_v T}{8\pi} \right)^{1/2}, \tag{4}$$

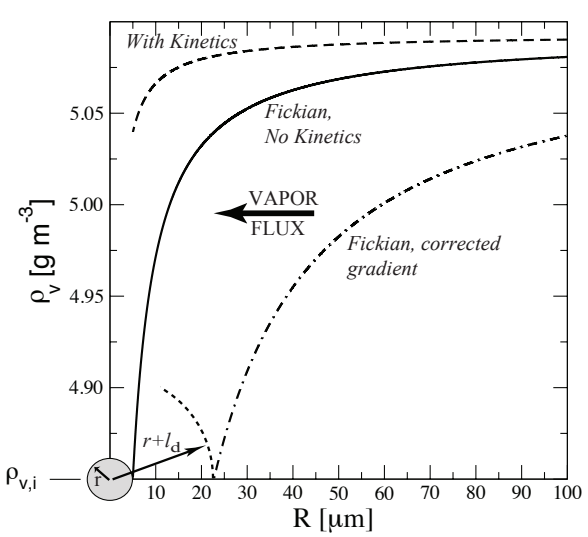

Figure 1: Density profile as a function of radial distance from the surface of an ice sphere for T = 268.15K, s_i = 5%, and α_d = 0.01. The aolid line is the classical Fickian vapor profile, the dashed line is the vapor profile for kinetically-limited growth, and the dash-dot line is the Fickian vapor profile for a drop of size $r + l_d$.

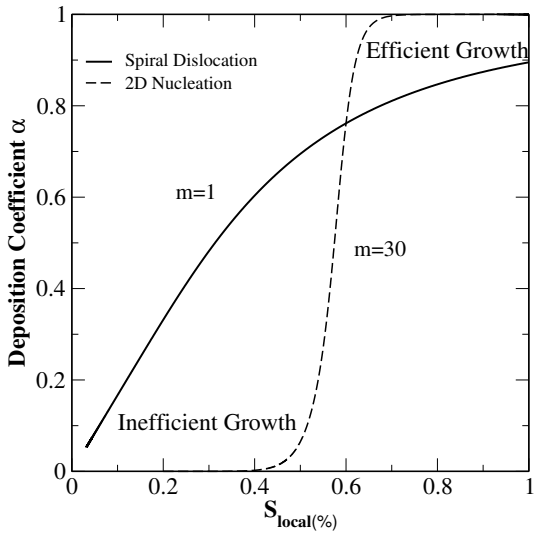

Figure 2: Deposition coefficient changes with local supersaturation

for the vapor kinetic length, and

$$l_T = \frac{4K_T}{\alpha_T \rho_a c_p \overline{v}_a} \qquad \text{where} \qquad \overline{v}_a = \left(\frac{R_d T}{8\pi}\right)^{1/2} \tag{5}$$

for the thermal kinetic length. $\overline{v}_v$ is the mean speed of a vapor molecule, and $\overline{v}_a$ is the mean speed of an "air" molecule. As α_T is thought to be near one, its impacts on growth are relatively minor and we do not attempt to parameterize its influence in this paper.

These length scales prove useful for parameterizing α_d. The form of Eq. 3 suggests that this is the case as r/l_d appears in the modified diffusion coefficient. However, one may also interpret l_d as the length-scale necessary to correct the classical, Fickian, vapor gradient for the influences of surface kinetics. For instance, Fig. 1 shows the profile of vapor density with distance away from the surface of an ice sphere. Classical, Fickian, diffusive growth indicates that the surface should be at the equilibrium value. However, when surface kinetics are included, vapor uptake at the surface is reduced leading to a rise in the vapor density near the surface. A simple analysis shows that when $r + l_d$ is used as an effective size, the vapor flux is identical to that in the kinetically-limited case. This is shown as a corrected gradient in Fig. 1. We can therefore assume that l_d, which is proportionally dependent on the deposition coefficient, can be considered the vapor jump length, and may be further parameterized for non-spherical cases.

3 Surface Kinetic Effects for Spheroidal Growth

The use of spheroidal particles allows for more generality when describing crystal shapes. Of course, spheroidal crystals do not occur in nature, however a spheroid allows for the prediction of two crystal lengths, the a and c axes, unlike a sphere which only allows for the prediction of the radial dimension. While spheroids are a rough, first order approximation to the shapes of real crystals, the ability to predict two axis lengths has the advantage that crystal aspect ratios can be predicted, habits can evolve naturally, and better predictions of cloud ice mass are possible since some of the non-linearities in crystal growth can be captured (e.g. Chen and Lamb, 1994; Sulia et al., 2010). A further advantage of using spheroidal particles is that predicting an a and c axis allows the use of laboratory-measured deposition coefficients for these two axes. Some measurements present a particle averaged deposition coefficient, which is useful for spherical particles, but many measurements provide data for growth efficiencies along the a and c axes. Hence, traditional methods for including the deposition coefficient for spherical particles cannot easily make use of these data. Nevertheless, it is possible to modify the spheroidal growth model of Chen and Lamb (1994) so that the deposition coefficients for each axis length is predicted.

3.1 Prediction of Deposition Coefficients

To predict the deposition coefficient along a particular axis, we use the parameterization provided by Nelson

and Baker (1996) and Lamb and Chen (1995). They suggest that α_d can be calculated in a general way for both molecular incorporation mechanisms: 2-D nucleation and spiral dislocation growth. According to classic ice crystal growth theories (Burton et al., 1951), the molecular incorporation on the ice surface normally is considered in two ways. The difference comes from the origin of the steps on the ice surface, whether they result from two-dimensional (2-D) nucleation or from the emergence of screw dislocations on the growing surface. An single expression for α_d that captures the main physics of both growth mechanisms is,

$$\alpha_d = \left(\frac{S_{local}}{S_{crit}}\right)^m tanh\left[\left(\frac{S_{crit}}{S_{local}}\right)\right]^m \quad (6)$$

where m is an adjustable parameter that represents the growth mechanisms, S_{local} is the supersaturation just above the crystal's axis, an S_{crit} is the critical supersaturation for the initiation of growth along the axis. The m value is somewhat arbitrary and is adjusted so that α_d matches theory and lab-based knowledge of crystal growth. Spiral dislocations result from a permanent ledge defect in the crystal face, and so growth occurs at all supersaturations. As shown in Fig. 2, a value of $m = 1$ produces a continual rise in α_d with supersaturation, and matches the theoretical functional dependence of Burton et al. (1951). In contrast, 2-D nucleation requires a specific supersaturation over the crystal face (critical supersaturation, S_{crit}) before a two-dimensional "island" is formed. An m value of 30 produces a very sharp increase in α_d at S_{crit}, indicating a rapid transition from nearly zero growth of the crystals axis to growth.

Most laboratory data on crystal growth provide values of the critical supersaturations for the crystal faces (e.g. Nelson and Baker, 1996; Libbrecth, 2003), and so deposition coefficients can be predicted for each face (basal and prism). In our analysis that follows, we make the assumption that these data can be used to describe the efficiency of growth of the a and c-axes of a spheroid. Although this is a first-order assumption, the method is able to reproduce some of the results of highly accurate crystal growth models.

3.2 Spheroidal Growth Model

In order to further explore the complexity of the crystal growth and to look at the feedback between the primary habit and the surface kinetics, we present a self-consistant theory to calculate the mass growth rate of spheroidal crystals. This theory is advantageous in many ways: First, it makes use of the two separate, but interrelated methods (as we discuss below). Second, diffusion of vapor toward the particle occurring within a small vapor jump length of the surface is computed using the traditional capacitance model for crystal growth. Third, the effects of surface kinetics are included in a similar fashion to that for spherical drops. For non-spherical particles we allow for the prediction of different deposition coefficients for each crystal axis (a and c) depending on the vapor flux over each axis based on crystal growth theory (see Fig. 3 and Sulia et al., 2010). Matching the total mass flow toward the particle from both theories yields a modified Fickian-distribution model of spheroidal crystal growth that is consistent with surface kinetics.

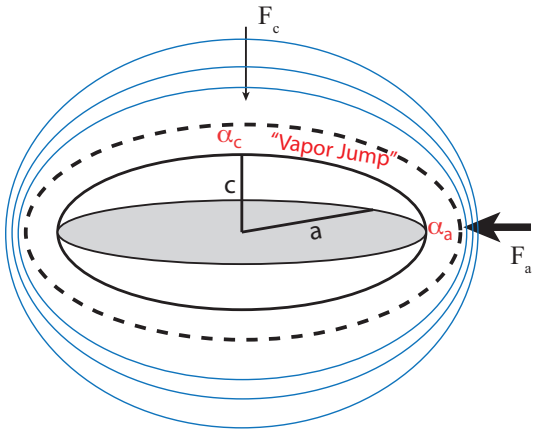

Figure 3: Cartoon depicting surface kinetic modifications to Chen and Lamb's (1994) habit evolution model. The diffusive flow of mass in the a and c directions (F_a and F_c respectively) is matched with kinetic theory along the same directions. As in the spherical theory, the fluxes are reduced by respective deposition coefficients along each direction leading to a kinetically-modified rate equation. The deposition coefficients along a and c (α_a and α_c, respectively) are predicted using data for the critical supersaturation along each direction.

The mathematics behind the theory are rather involved and have been left out for brevity. The main approach consists in keeping the growth rate equation the same as Eq. 1 where the capacitance is a function of the a and c-axis lengths. However, the combined vapor and thermal diffusion coefficient, G, has a similar form as Eq. 2 but is revised to include the geometry of a spheroid and the vapor jump length surrounding the particle for both crystal faces (Fig. 3). The deposition coefficents along each axis direction (a and c), α_a and α_c, are predicted using laboratory-derived data for the critical supersaturations, and follow the method described in Lamb and Chen (1995).

An advantage of this new method is that it is able to capture the feedback between the primary habit of the crystal and the deposition coefficient along each axis direction. Rather than calculating the average flux and deposition coefficient over the particle as in the spherical growth model, we are able to predict separate fluxes and deposition coefficients for both the a and c-axes and relate them consistently with the *mass distribution hypothesis* of Chen and Lamb (1994). This is possible because the Chen and Lamb (1994) model uses the vapor fluxes along the a and c axes in its explicit formulation. Consequently, deposition coefficients along these axes can be

predicted and combined with the vapor fluxes from the model (see Sulia et al., 2010) using ideas from crystal growth theory (e.g. Nelson and Baker, 1996) to produce a model that is more appropriate under low supersaturation conditions which produce weaker growth. In addition, our method is very flexible. We can use either an average value of the deposition coefficient for the particle, something that is often measured in the lab (e.g. Magee et al., 2006), or we can make use of the observational data for critical supersaturation on the prism and basal faces derived through other measurements such as (Nelson and Baker, 1996) and (Libbrecth, 2003).

As with any model or theory, ours has limitations that should be borne in mind. First, computing the diffusion rate to the particle based on the capacitance model is a limitation. The capacitance model has the wrong surface boundary condition for faceted crystal growth: The vapor density over the particle surface is a constant whereas in faceted growth the fluxes over the faces are, *on average*, constant. This feature of the capacitance model causes the aspect ratio to remain constant during crystal growth. Consequently, the capacitance model breaks down for both faceted growth and for crystal growth in general (since aspect ratios are not constant). Nevertheless, the capacitance model can be made to work well at water saturation if it is modified so that it accounts for the flux distribution along the a and c axes using crystal growth theory as is done by Chen and Lamb (1994). This modification results in a combined diffusion-crystal growth model (retermed the Fickian-distribution model by Sulia et al., 2010) that is more accurate for atmospheric applications than the pure capacitance model. A second limitation is the use of spheroids to represent crystals. Of course, real crystals are never spheroids. However, it is important to keep in mind that an ice growth model that is developed for atmospheric applications must necessarily be simple. A spheroid is an improvement over a sphere in the sense that two axes can be predicted, along with the aspect ratio of the particle, allowing for the evolution of primary habits. Moreover, by including a reduced density for spheroidal growth and sublimation (e.g. Sulia et al., 2010), particles other than hexagonal prisms can be modeled at least to first order. Using a spheroid, then, allows for the modeling of a larger range of particle types including irregular crystals.

4 Model Results

To investigate the link between surface kinetic resistance and macroscopic crystal properties, we run our new model in both a single-particle framework in which only crystal size changes in time, and a Lagrangian parcel model framework. Both models are run over a range of parameter values under atmospheric conditions. We begin with single particle simulations and then use these to understand the Lagrangian parcel model studies that follow.

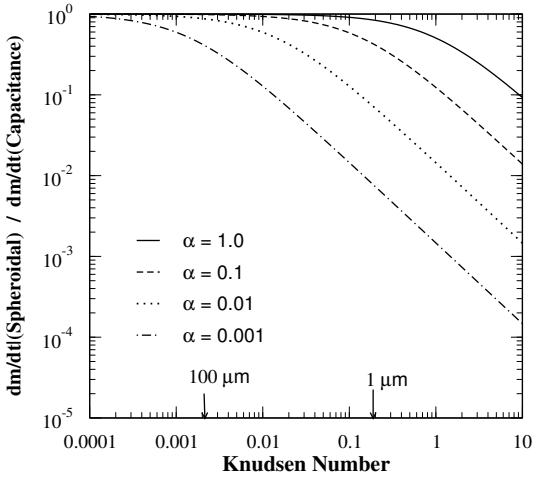

Figure 4: The Knudsen number dependence of the flux ratio of the spheroidal growth model and the capacitance model, given constant deposition coefficients on both growth direction and $\alpha_a = \alpha_c = \alpha$.

4.1 Single Particle Simulation

To understand the physical essence of including surface kinetics in ice crystal growth, we examine how individual particles react to varying environmental parameters, and their effects on, and feedbacks with, the deposition coefficients. Current cloud models generally approximate the rate of mass growth of a crystal ($\frac{dm}{dt}$) via the capacitance model in which crystals are assumed to be spheres or simple shapes. These models are also apt to neglect the treatment of surface kinetics. We improve these methods by combining the capacitance model and the *mass redistribution hypothesis* (i.e. the Fickian-distribution model Chen and Lamb, 1994; Sulia et al., 2010) with the deposition coefficients described above.

It is important to note the level of accuracy demonstrated by our model in comparison to the detailed growth model developed by Wood et al. (2001). Their method is based on solving the Laplace equation on a triangular grid over a hexagonal-shaped ice crystal which includes predictions of the deposition coefficients over the crystal faces. Although this detailed model is computationally expensive and is not suitable for implementation into cloud models, it is a relatively accurate standard to which we can compare. The comparison is limited in the sense that only hexagonal prisms are modeled, not other types of atmospheric crystals. In sum, we compare the instantaneous mass growth of the above three models: the capacitance model, our spheroidal growth model, and the detailed hexagonal growth model of Wood et al. (2001) for the two growth mechanisms (2-D nucleation and spiral dislocation).

4.1.1 Knudsen Number Dependence

First, to determine the conditions when the surface kinetic effect is important to spherical particles, we use the dimensionless Knudsen number, K_n. The Knudsen number is useful for determining whether diffusion or surface kinetics dominate growth. In our case K_n is the ratio of the diffusion rate which scales with D_v and the molecular exchange at the surface which scales with $\frac{1}{3}r\overline{v}_v$, where D_v is the gas phase diffusion coefficient, $\overline{v}_v$ is the averaged molecular speed and r is the size which is the particle radius for a sphere. This leads to the classical relationship,

$$K_n = \frac{3D_v}{r\overline{v}_v} \tag{7}$$

which is commonly used (Kulmala and Wagner, 2001). Large Knudsen number ($K_n \gg 1$, small particles) corresponds to diffusion limited growth, in which the mass flux is based on Fick's law. In this case, the mass growth rate can be represented by the capacitance model. A Knudsen number of $K_n \sim 1$ means both diffusion and surface kinetics are important in the vapor transport. Small Kundsen number ($K_n \ll 1$, large particles) corresponds to kinetically limited growth, in which surface resistance actively limits the vapor uptake by the particle. For relatively small Kundsen numbers, the diffusive mass flux should be modified by a correction factor associated with the deposition coefficient, as in the spherical growth model. In Fig. 4, we show the Knudsen number dependence of the correction factor, where we assume the particles are spherical so the deposition coefficient has one value. The magnitude of correction depends on the deposition coefficient and K_n. For particle size ranging from 1 to 100 μm, the kinetically modified mass flux deviates significantly from the pure Fickian flux when $\alpha < 0.1$. Lab measurements show that the deposition coefficient can reach values as low as 0.005 (Magee et al., 2006).Therefore, it is critical to provide a method to correct the mass flux from capacitance model for surface kinetic effects.

4.1.2 Effects of Crystal Shapes

The above discussion is based on spherical particles, however the shapes of the crystals ($\Phi = c/a$) influence the growth rate and the surface kinetics as well. Fig. 5 shows the effect of crystal shape on the predicted mass growth rates for three growth models. Note that the variation in mass growth rate with aspect ratio is proportional to the crystal capacitance. When crystals are isometric, the growth rates are at a minimum, while rapid growth occurs for crystals with extreme shapes. This change in growth with aspect ratio occurs because the larger vapor gradient over the sharp crystal edges provides an efficient sink of vapor molecules. The capacitance model over-predicts the mass growth rates by a large amount when compared to the curves from Wood et al. (2001) and our spheroidal growth model, and this is especially true for 2-D nucleation growth. Note that

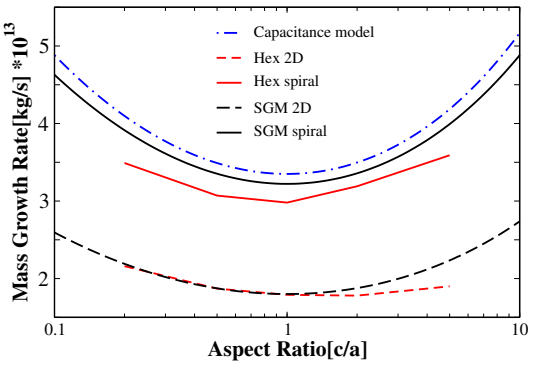

Figure 5: Comparison of mass growth rates predicted by the spheroidal model using two growth mechanism: 2-D nucleation (black dashed line) and spiral dislocation (black solid line) , and by the capacitance model (blue dash-dot line). These results are plotted with the hexagonal model results produced by Wood et al. (2001), red dashed line for 2-D nucleation and red solid line for spiral dislocation. The ambient conditions used here were T = 268.15K, S_i = 1%, p=500 mbar, the crystal mass m=8×10^{-10}kg.

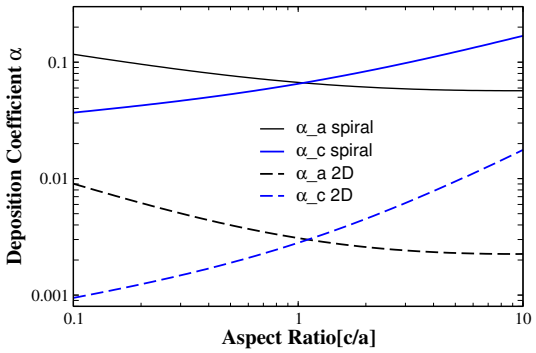

Figure 6: Predicted deposition coefficient α_a and α_c with changing aspect ratio. We assumed $S_{crit,a}$= 0.55%, $S_{crit,c}$=0.58% .

the spheroidal model compares well with the detailed hexagonal growth model for both growth mechanism. However, compared with the detailed model, our model results over-predict the mass growth rates for spiral dislocation growth and for columns with 2-D nucleation growth. The maximum deviation is about 25%.

The mass growth rates in Fig. 5 uses the predicted values of α along both a and c axis. Fig. 6 shows the value of the predict deposition coefficient on both the a and c axes, using the lab derived critical supersaturation $S_{crit,a}$= 0.55%, $S_{crit,c}$=0.58% . Spiral growth gives higher deposition coefficient than 2-D nucleation growth as expected. Columnar growth produces a deposition

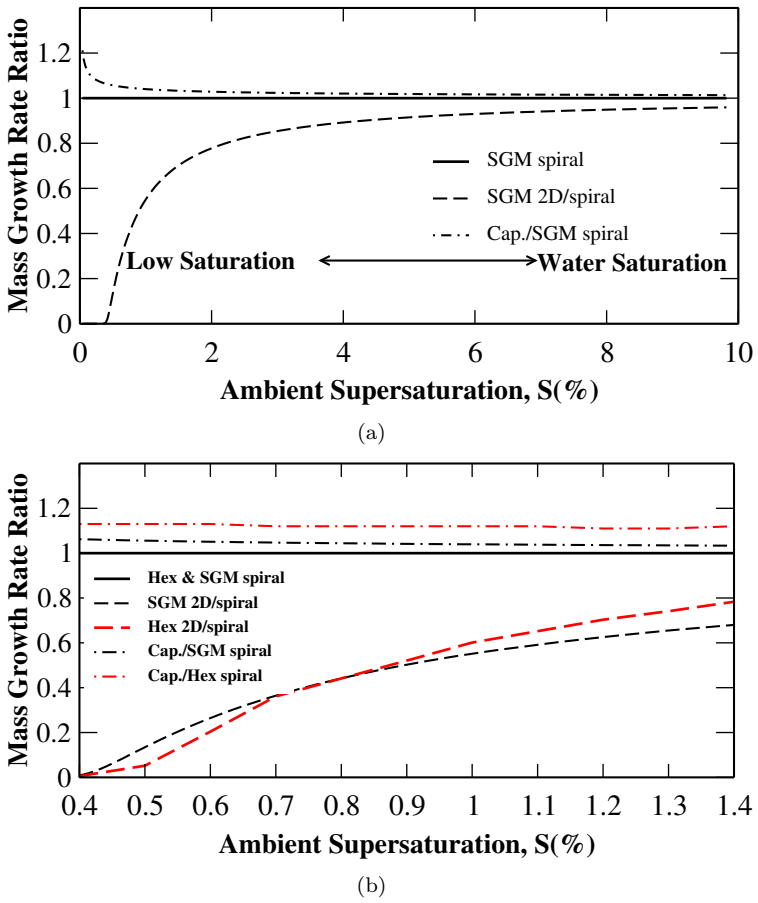

Figure 7: The effect of changing the supersaturation for isometric crystals, all the mass growth rates all ratioed to the spiral growth rate . (a) shows the model results from our spherical growth model with the ambient supersaturation from low value to water saturation. (b) is a zoom in plot for low supersaturation region of (a) and plot the SGM results (black lines) on top of the detailed model results (Wood et al., 2001) (red lines). The ambient conditions used here were T = 268.15K, p=500 mbar, the crystal mass m=8×10^{-10}kg, and the spherical crystal radius = $59\mu m$.

coefficient on c axis (α_c) that is larger than that on the a axis (α_a). During plate growth, the deposition coefficient on a axis (α_a) exceeds that on the c axis (α_c). Note that the crossing points for α_c and α_a are not at an aspect ratio of one, and this is due to unequal values of the critical supersaturation along the a and c direction. In our case, $S_{crit,a} < S_{crit,c}$, the surface resistance on a axis is less then that on c axis, therefore we have larger α_a for isometric particles.

4.1.3 Ambient Supersaturation Dependence

In this section, we examine the dependence of kinetically reduced growth on the ambient supersaturation. At liquid saturation, the crystal vapor growth is mainly limited by gas diffusion and the capacitance model holds in these conditions. At low supersaturation, the vapor density of the environment is much lower and only a small fraction of the vapor molecules impinging on the particle surface can be incorporated into the ice crystal. Therefore, surface resistance has to be taken into account. As we see in Fig. 7, by considering surface processes, the mass growth rates are reduced for situations in which the supersaturations are relatively low, from 0 to a few percent. This is especially true for 2-D nucleation. At water saturation the SGM results have the trend to approach to the capacitance model result. It is well known that large errors occur when surface kinetics through 2-D nucleation is neglected at low supersaturations, and this is shown in Fig. 7(b). By comparing our model results with the detailed hexagonal model of Wood et al. (2001), we note a similar mass growth ratio trend at low supersaturation, except we have a smaller ratio of capacitance growth rate to spiral growth rate. This means our spiral growth model over predict the growth rate when compared to the detailed model, which agrees with what we show in Fig. 5

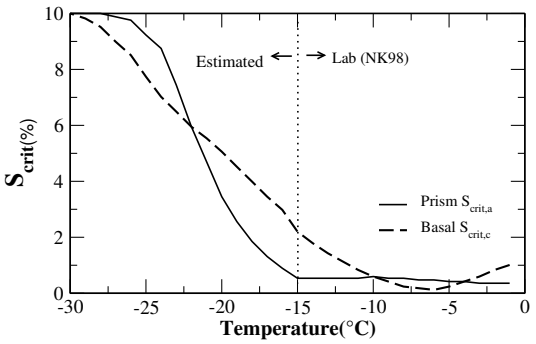

Figure 8: The temperature dependence of ice particle surface property $S_{crit,a}$ and$S_{crit,c}$, regenerated from Wood et al. (2001). For T > -15 °C, our model uses measurements from Nelson and Knight (1998). For lower temperatures, those values are from field experiments estimated by Wood et al. Note that these values are all for 2-D nucleation growth mechanism.

4.2 Parcel Model Simulation

To further examine the potential accuracy of our spheroidal growth method, we implemented it into a Lagrangian parcel model framework and compare these results with those of the classical capacitance model and the detailed hexagonal model. The parcel model simulations follow those conducted by Wood et al. (2001). Comparing our model to the simulations of Wood et al. (2001) in a more realistic cloud situation provides a more robust test of our theory since temperature, pressure, and supersaturation all vary in time. The simulations are run for a warmer case (initial T = -13 °C) and a colder case (initial T = -25 °C). For each case, we use the same initial atmospheric parameters (i.e. temperature, ice supersaturation and vertical velocity) and particle properties (i.e. particle size, number concentration). Data for the critical supersaturation over the a and c-axes are available from laboratory measurements (Nelson and Knight (1998)) for temperatures 0 to -15 °C and derived values from Wood et al. (2001). for temperatures -15 to -30 °C. These are used in our model simulations, and linear interpolation is used to approximate the critical supersaturation between data points.

We begin by discussing the warmer cloud case in which the parcel is lifted over 1200 seconds (Fig. 9). The ambient temperature of the parcel decreases rapidly in the first 200 seconds and this decrease is slowed due to depositional warming. This result corresponds with the total mass growth which is initially slow, therefore less latent heating occurs. Additionally, these variations are consistent with the supersaturation evolution. The ice supersaturation increases due to vertical lifting and parcel cooling until the crystals are large enough to become an effective sink of vapor. The latent heating that occurs through vapor deposition leads to a slower decrease in temperature at higher altitudes in the cloud. The new spheroidal growth model compares well to the detailed hexagonal model in all cases excluding that for 2-D nucleation. In that case, a lower temperature and mass results but a much higher supersaturation. This shows that the spheroidal growth model produces greater surface resistance than the hexagonal model in low ice saturation (i.e. 0.5%) conditions.

In the cold case (Fig. 10), the parcel rises at 35 $cm\,s^{-1}$ with an initial temperature of T=-25°C, and an initial ice supersaturation of $S_i = 25\%$. A larger initial supersaturation is used so that the crystals take up the excess vapor quickly at the start of the simulation and reaches quasi-equilibrium after approximately 100 seconds. The latent heating caused by the early rapid growth overcomes the cooling due to vertical motion which leads to a temperature increase within the first few minutes. However, after this time the temperature decreases and continues to drop with time. The spheroidal growth model produces trends similar to that of the hexagonal model in the evolution of temperature, supersaturation, and total ice mass.

The predicted shape evolution is substantially different for each growth model, and this indicates a possible limitation of our method. In both the warm and cold cases, the hexagonal model evolves a different aspect ratio (Φ) as compared to our spheroidal model for each growth mechanism. The hexagonal model produces extreme-shaped plates and columns for 2-D nucleation growth with Φ values of approximately 0.07 for the warm case and 7.0 for the cold-case simulation. For the case of spiral dislocation growth, Φ is approximately 1.0 for both cases. The aspect ratios predicted by the spheroidal growth model are not sensitive to the growth mechanism, and their values are more close to that from capacitance model. The reason for the differences between the models is not completely clear, but it appears to be due to the fact that the hexagonal model allows for the cessation of growth along a given direction, whereas the spheroidal growth model always grows crystal in both directions. Another reason for the differences is that the *mass distribution hypotheses* used by Wood et al. (2001) and Chen and Lamb (1994) differ. The hexagonal results of Wood et al. (2001) uses the hypothesis put forth by Nelson and Baker (1996), whereas our model uses the hypothesis of Chen and Lamb (1994). This difference could lead to contrasting aspect ratio evolution, and hence to varying crystal mass evolution. We have tested our model by using Nelson and Baker (1996) hypothesis, and got a better match with the detailed hexagonal model results for aspect ratio evolution. However, it is difficult to determine the relative accuracy of the hypotheses, as both methods have the backing of empirical data. As a result, further laboratory studies are required to critically examine the growth hypotheses and constrain our numerical model.

Acknowledgments. The authors would like to thank the National Science Foundation for support under Grant ATM-0639542. The authors are indebted to Kara Sulia for her careful editing of the scientific content of this article.

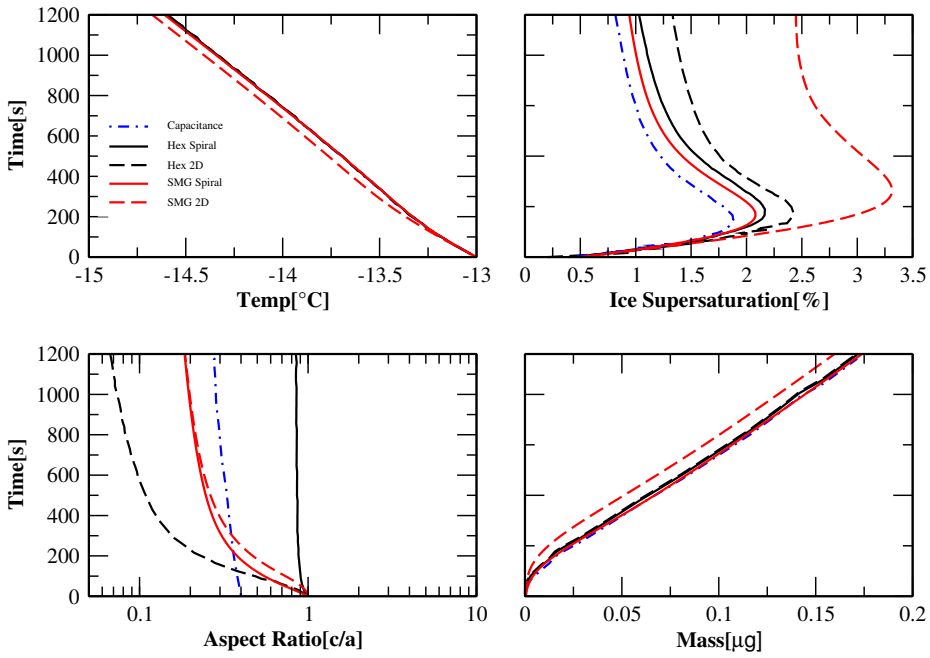

Figure 9: Evolution of ambient conditions and crystal properties for parcel model simlations of an ice cloud. The model uses a vertical velocity of w=20 cm/s, particle number concentration N =$10^6 m^{-3}$, and P=500 mb. Comparison between the three ice crystal growth models: spheroidal model (red curves) and hexagonal model (black curves) and the capacitance model(blue dash-dot line). Results for 2-D nucleation (dashed line) and spiral dislocations (solid line) are shown for the spheriodal and hexagonal models. The critical supersaturation along each axis was kept constant and the same ($S_{crit,a}$=$S_{crit,c}$=1%) for both 2-D nucleation and spiral growth.

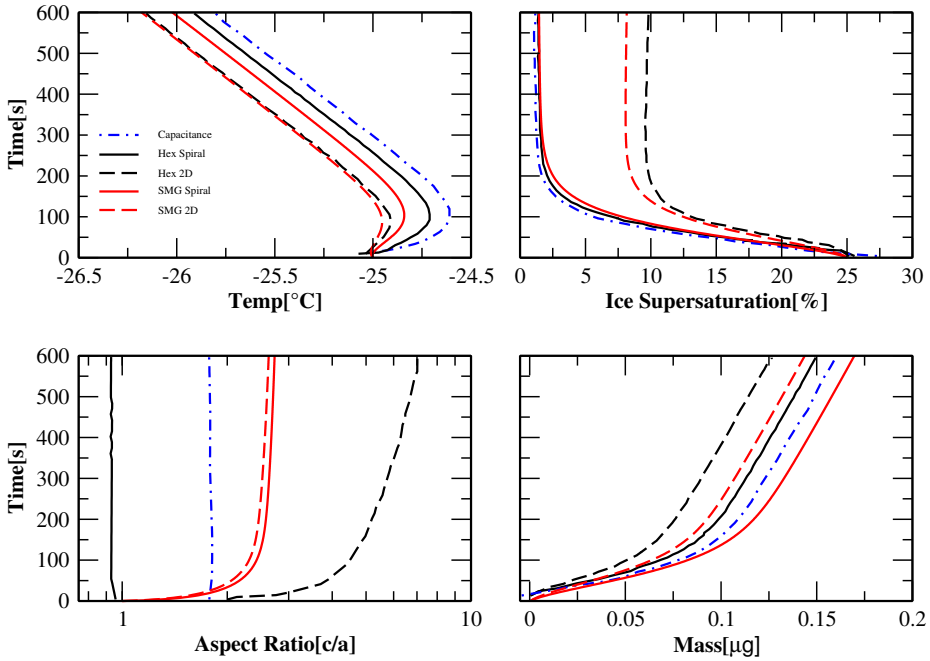

Figure 10: Same format as Fig. 9 for cloud condition, w=35 cm/s, N =$10^6 m^{-3}$, P=330 mb. The values used for the ice surface parameters were $S_{crit,c}$=8%, $S_{crit,a}$=9% for 2-D nucleation and $S_{crit,a}$= $S_{crit,c}$=2%.

References

Avramov, A. and J. Harrington, 2010: The influence of parameterized ice habit on simulated mixed-phase arctic clouds. *J. Geophys. Res.*, **115**, D03 205, doi: 10.1029/2009JD012108.

Bailey, M. and J. Hallett, 2002: Nucleation effects on the habit of vapour grown ice crystals from -18 to -42°c. *Quart. J. Roy. Meteor. Soc.*, **128**, 1461–1483.

Bailey, M. and J. Hallett, 2004: Growth rates and habits of ice crystals between -20o and -70°c. *J. Atmos. Sci.*, **61**, 514–544.

Bailey, M. and J. Hallett, 2009: A comprehensive habit diagram for atmospheric ice crystals: Confirmation from laboratory, airs ii, and other field studies. *J. Atmos. Sci.*, **66**, 2888–2899.

Burton, W. K., N. Cabrera, and F. C. Frank, 1951: The growth of crystals and the equilibrium structure of their surfaces. *Philosophical Transactions of the Royal Society of London. Series A, Mathematical and Physical Sciences*, **243 (866)**, 299–358.

Chen, J. and D. Lamb, 1994: The theoretical basis for the parameterization of ice crystal habits: Growth by vapor deposition. *J. Atmos. Sci.*, **51**, 1206–1221.

Fukuta, N. and T. Takahashi, 1999: The growth of atmospheric ice crystals: A summary of findings in vertical supercooled cloud tunnel studies. *J. Atmos. Sci.*, **56**, 1963–1979.

Gayet, J.-F., et al., 2002: Quantitative measurement of the microphysical and optical properties of cirrus clouds with four different in situ probes: Evidence of small ice crystals. *Geophys. Res. Let.*, **29(24)**, 2230, doi: 10.1029/2001GL0014342.

Harrington, J. Y., R. Carver, and D. Lamb, 2009: Parameterization of surface kinetic effects for bulk microphysical models: Influences on simulated cirrus dynamics and structure. *J. Geophys. Res.*, **114**, D06 212, doi: 10.1029/2008JD011050.

Harrington, J. Y., T. Reisin, W. R. Cotton, and S. M. Kreidenweis, 1999: Cloud resolving simulations of Arctic stratus. Part II: Transition-season clouds. *Atmos. Res.*, **51**, 45–75.

Hashino, T. and G. J. Tripoli, 2007: The spectral ice habit prediction system (SHIPS). Part I: Model description and simulation of the vapor deposition process. *J. Atmos. Sci.*, **64**, 2210–2237.

Hashino, T. and G. J. Tripoli, 2008: The spectral ice habit prediction system (SHIPS) Part II: Simulation of nucleation and depositional growth of polycrystals. *J. Atmos. Sci.*, **65**, 30713094.

Khvorostyanov, V., H. Morrison, J. Curry, D. Baumgardner, and P. Lawson, 2006: High supersaturation and modes of ice nulceation in thin tropopause cirrus: Simulations of the 13 July 2002 cirrus regional study of tropical anvils and cirrus layers case. *J. Geophys. Res.*, **111, D02201**, doi:doi:10.1029/2004JD005235.

Korolev, A., G. Isaac, and J. Hallett, 1999: Ice particle habits in arctic clouds. *Geophys. Res. Let.*, **26**, 1299–1302.

Kulmala, M. and P. E. Wagner, 2001: Mass accommodation and uptake coefficients – a quantitative comparison. *Journal of Aerosol Science*, **32 (7)**, 833 – 841, doi:DOI: 10.1016/S0021-8502(00)00116-6.

Lamb, D. and J. Chen, 1995: An expanded parameterization of growth of ice crystals by vapor deposition. *Conference on Cloud Physics*, Dallas, Texas, AMS, Boston, 15-20 January, 389-392.

Libbrecth, K., 2003: Growth rates of the principal facets of ice between -10°C and -10°C. *J. Crystal Growth*, **247**, 530–540.

Liu, H.-C., P. Wang, and R. Schlesinger, 2003: A numerical study of cirrus clouds. Part II: Effects of ambient temperature, stability, radiation, ice microphysics, and microdynamics on cirrus evolution. *J. Atmos. Sci.*, **60**, 1097–1119.

Magee, N., A. Moyle, and D. Lamb, 2006: Experimental determination of the deposition coefficient of small cirrus-like crystals near -50 °C. *Geophys. Res. Let.*, L17813, doi: 10.1029/2006GL026665.

Mordy, W., 1959: Computations of the growth by condensation of a population of cloud droplets. *Tellus*, **11**, 17–44.

Nelson, J., 1994: A Theoretical Study of Ice Crystal Growth in the Atmosphere. Ph.D. thesis, University of Washington, 183pp.

Nelson, J. and M. Baker, 1996: New theoretical framework for studies of vapor growth and sublimation of small ice crystals in the atmosphere. *J. Geophys. Res.*, **101**, 7033–7047.

Nelson, J. and C. Knight, 1998: Snow crystal habit changes explained by layer nucleation. *J. Atmos. Sci.*, **55**, 1452–1465.

Pruppacher, H. R. and J. D. Klett, 1997: *Microphysics of Clouds and Precipitation*. Kluwer Academic Publishers, Boston, 954 pp.

Starr, D. O. C. and Co-authors, 2000: Comparison of cirrus models: A project of the GEWEX cloud system study group (GCSS) working group on cirrus cloud systems. *13th International Conf. on Clouds and Precipitation*, Reno NV, ICCP, 1–4.

Starr, D. O. C. and S. Cox, 1985a: Cirrus clouds. Part I: A cirrus cloud model. *J. Atmos. Sci.*, **42**, 2663–2681.

Starr, D. O. C. and S. Cox, 1985b: Cirrus clouds. Part II: Numerical experiments on the formation and maintenance of cirrus. *J. Atmos. Sci.*, **42**, 2682–2694.

Sulia, K., J. Harrington, and H. Morrison, 2010: The parameterizaiton of primary ice habit for bulk models: Influences on mixed-phase cloud glaciation. *13^{th} Conference on Cloud Physics*, Portland, OR, American Meteorological Society.

Takahashi, T., T. Endoh, G. Wakahama, and N. Fukuta, 1991: Vapor diffusional growth of free-falling snow crystals between -3 and -23°c. *J. Meteorol. Soc. Japan*, **69**, 15–30.

Wood, S., M. Baker, and D. Calhoun, 2001: New model for the vapor growth of hexagonal ice crystals in the atmosphere. *J. Geophys. Res.*, **106**, 4845–4870.